[Downloaded from www.aece.ro on Thursday, July 03, 2025 at 19:04:12 (UTC) by 172.69.214.181. Redistribution subject to AECE license or copyright.]

Boost Converter with Active Snubber Network

Felix A. HIMMELSTOSS[1], Ali Rıza DERIN[2], Mihai CERNAT[2]
[1]*University of Applied Sciences Technikum Vienna, Austria,* [2]*Karabük University, Turkey*
mihaicernat@yahoo.com

***Abstract*—A new concept for reducing the losses in a boost converter is described. With the help of an auxiliary switch and a resonant circuit, zero-voltage switching at turn-off and zero-current switching during turn-on are achieved. The modes of the circuit are shown in detail. The energy recovery of the turn-off is analyzed and the recovered energy is calculated; an optimized switching concept therefore is described. The influence of the parasitic capacity of the switch is discussed. Dimensioning hints for the converter and the design of the recuperation circuit are given. A bread-boarded design shows the functional efficiency of the concept.**

***Index Terms*—snubbers, active circuits, switching converters, zero current switching, zero voltage switching.**

I. INTRODUCTION

There are numerous papers about the boost converter and methods to decrease the losses. Basics of the boost converter are described e.g. in [1, 2]. A very well-known method to reduce the losses is the quasi-resonant converter concept [3-5]. We distinguish zero-current ZC quasi-resonant and zero-voltage ZV quasi-resonant converters. Other concepts are the zero voltage and the zero current transition concept or combinations of them [6-24].

In this paper we use an active snubber concept, based on the network described in [21] to reduce the losses. The active switch turns on with zero current switching ZCS and turns off with zero voltage switching ZVS. The energy used for this soft switching is fed into the output by a recuperation circuit with low losses. The tasks of the snubber are: to reduce turn-off switching loss and to define the dv/dt ratio during turn off. Due to new very fast active switching elements, the second one becomes more important (to reduce problems with EMC).

II. CIRCUIT OPERATION

The boost converter (Fig. 1) consists of the coil L, the active switch S, the free-wheeling diode D, and the output capacitor C. The snubber consists of the inductor L_E (to reduce the velocity of the current during turn on), the capacitor C_E (to reduce the losses across the switch S during turn off and to reduce the overvoltage across the switch), the snubber diode D_E, the diode D_U, the inductor L_U, the auxiliary switch S_U, and the feedback diode D_R (to transfer the energy of the snubber capacitor C_E to the output). The load is represented by a resistor. U_{in} is the input voltage, U_{out} is the output voltage.

Inductance L is large compared to L_E, capacitance C is large compared to C_E. For the analysis, we replace the converter coil L by a current source I, and the output capacitor C by a voltage source U_{out}. Ideal elements are used.

In following, the functioning of the proposed boost converter with active snubber network will be described.

We can make a distinction between different seven time intervals, which we called Modes.

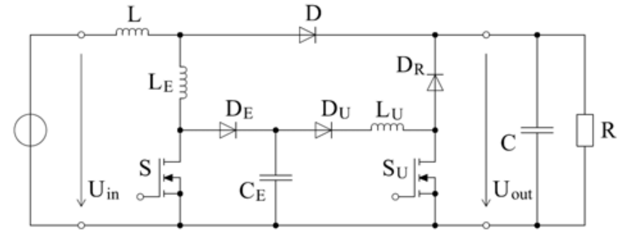

Figure 1. Boost converter with low-loss snubber network.

Mode 0 (Fig. 2): the active switch is on, the capacitor C_E is discharged. This is the normal on-state of the boost converter.

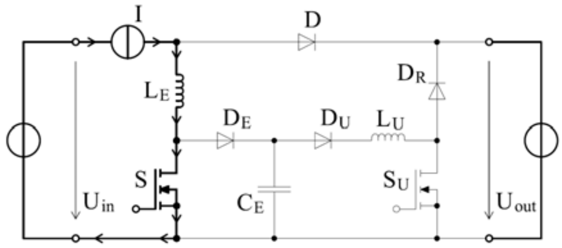

Figure 2. Turn-on state of the converter (mode 0).

Mode 1 (Fig. 3): at the beginning of this mode, the active switch S is turned off.

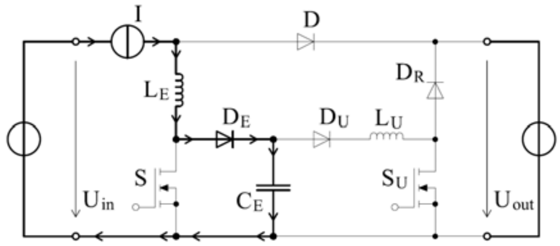

Figure 3. Start of the turn-off process (Mode 1).

The snubber diode D_E turns on and the current commutates into the snubber capacitor C_E. The capacitor voltage $u_{CE}(t)$ increases linearly according to

$$\frac{d\,u_{CE}}{d\,t} = \frac{I}{C_E}; \quad u_{CE}(0) = 0 \tag{1a, b}$$

$$u_{CE}(t) = \frac{I}{C_E} t \tag{2}$$

until it reaches U_{out}.

Mode 2 (Fig. 4): When the voltage across the capacitor C_E reaches U_{out}, the free-wheeling diode D turns on.

The energy in L_E continues to be transferred into C_E and a (little) part is now already transferred to the output. The circuit can be described by the state equations:

Digital Object Identifier 10.4316/AECE.2017.01008

1582-7445 © 2017 AECE

[Downloaded from www.aece.ro on Thursday, July 03, 2025 at 19:04:12 (UTC) by 172.69.214.181. Redistribution subject to AECE license or copyright.]

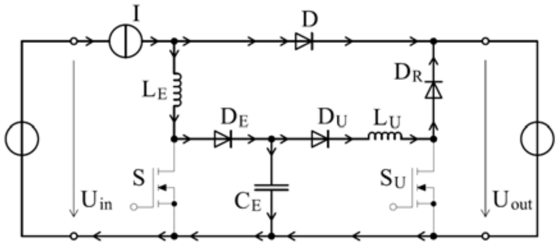

Figure 4. The free-wheeling diode turns on (Mode2).

$$\frac{di_{LE}}{dt} = \frac{U_{out} - u_{CE}}{L_E}; \quad i_{LE}(0) = I \tag{3a, b}$$

$$\frac{di_{LU}}{dt} = \frac{u_{CE} - U_{out}}{L_U}; \quad i_{LU}(0) = 0 \tag{4a, b}$$

$$\frac{du_{CE}}{dt} = \frac{i_{LE} - i_{LU}}{C_E}; \quad u_{CE}(0) = U_{out} \tag{5a, b}$$

This leads to:

$$i_{LE}(t) = \frac{L_E}{L_E + L_U} I \left(1 + \frac{L_U}{L_E} \cos \omega_2 t\right) \tag{6}$$

$$i_{LU}(t) = \frac{L_E}{L_E + L_U} I \left(1 - \cos \omega_2 t\right) \tag{7}$$

$$u_{CE}(t) = U_2 + \frac{I}{\omega_2 C_E} \sin \omega_2 t \tag{8}$$

where

$$\omega_2 = \sqrt{\frac{L_E + L_U}{C_E L_E L_U}}. \tag{9}$$

Mode 2 ends when the current i_{LE} reaches zero and the snubber diode D_E turns off. The voltage across C_E is now higher than the output voltage U_{out}.

Mode 3 (Fig. 5): the capacitor C_E and L_U form a resonant circuit.

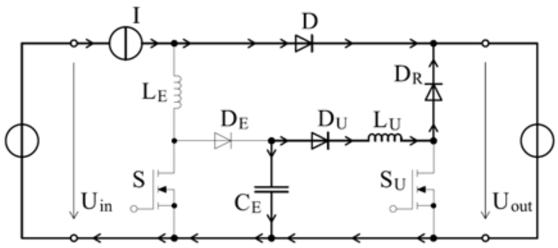

Figure 5. Resonance during the off-time (Mode 3).

If the voltage across C_E gets lower than U_{out} , the circuit goes again in Mode 2 with different initial conditions. There will be a ringing between these two modes until the voltage at C_E is stabilized to U_{out}. The circuit is described by:

$$\frac{1}{C_E}\int_0^t i_{LU} \cdot dt - u_{CE}(0) + L_U \frac{di_{LU}}{dt} + U_{out} = 0 \tag{10}$$

where $u_{CE}(0)$ is the voltage across C_E when Mode 3 begins.

Mode 4 (Fig. 6): this is the normal turn-off mode (free-wheeling mode) of the converter.

Mode 5 (Fig. 7): the main switch S is turned on again.

The current through the main switch S increases and the current through the free-wheeling diode D decreases

$$\frac{di_{LE}}{dt} = \frac{U_{out}}{L_E}; \quad i_{LE}(0) = 0 \tag{11a, b}$$

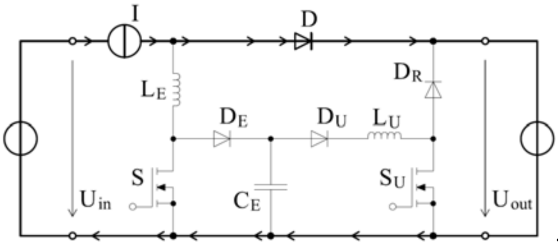

Figure 6. Turn-off state of the converter (Mode 4).

Mode 5 ends when the current I_{LE} reaches I. Then the current in the free-wheeling diode D is zero and it turns off. The main switch is now carrying the current I.

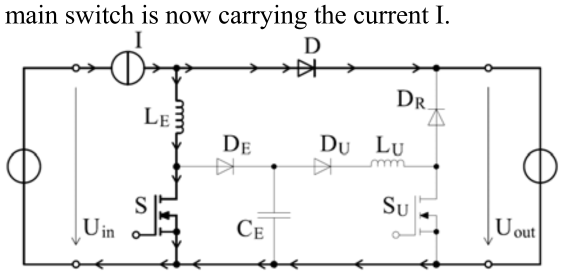

Figure 7. Beginning of the turn-on process (Mode 5).

Mode 6 (Fig. 8): The main switch is now carrying the current I and the auxiliary switch S_U is turned on (this switch can already be turned on synchronously to the main switch S, Mode 5).

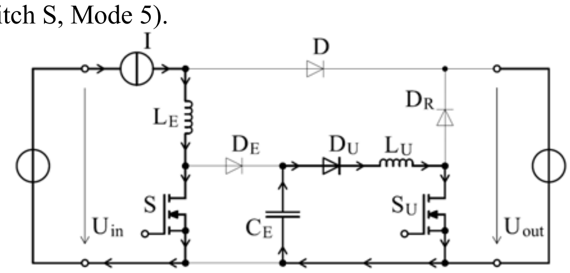

Figure 8. Resonant discharge of the snubber capacitor (Mode 6).

The right part of the circuit is now described by

$$\frac{di_{LU}}{dt} = \frac{u_{CE}}{L_U}; \quad i_{LU}(0) = 0 \tag{12a, b}$$

$$\frac{du_{CE}}{dt} = \frac{-i_{LU}}{C_E}; \quad u_{CE}(0) = U_{out} \tag{13a, b}$$

This leads to

$$i_{LU}(t) = U_{out}\ \omega_6\ C_E\ \sin \omega_6 t \tag{14}$$

$$u_{CE}(t) = U_{out}\ \cos \omega_6 t \tag{15}$$

where

$$\omega_6 = \left(C_E L_U\right)^{-1/2} \tag{16}$$

The capacitor C_E is discharged within a quarter of the period and the current reaches its maximum I_{LUmax} (Fig. 9):

$$I_{LUmax} = U_2\ \omega_6\ C_E \tag{17}$$

The duration of this process is:

$$T_6 = \frac{\pi}{2}\sqrt{C_E L_U} = \frac{\pi}{2}\frac{1}{\omega_6} \tag{18}$$

The capacitor voltage u_{CE} is now clamped to zero due to the snubber diode D_E. To feed back the energy, the auxiliary switch S_U has to be turned off.

[Downloaded from www.aece.ro on Thursday, July 03, 2025 at 19:04:12 (UTC) by 172.69.214.181. Redistribution subject to AECE license or copyright.]

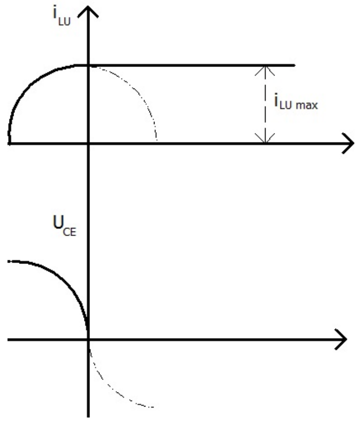

Figure 9. Current through the inductor L_U and voltage across the snubber capacitor C_E during Mode 6.

Mode 7 (Fig. 10): auxiliary switch S_U has turned off.

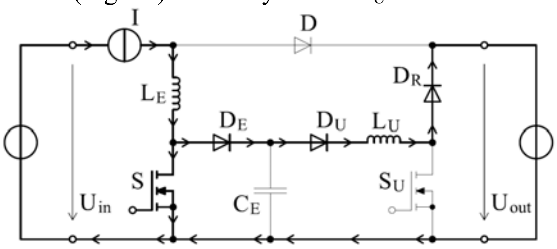

Figure 10. Recuperation (Mode 7).

The current i_{LU} decreases until the diodes turn off when the current reaches zero

$$\frac{di_{LU}}{dt} = \frac{-U_{out}}{L_U}; \quad i_{LU}(0) = I_{LUmax} \tag{19a, b}$$

The current decreases linearly according to

$$i_{LU}(t) = \frac{U_{out}}{L_U}\left(\sqrt{C_E L_U} - t\right) \tag{20}$$

The time for demagnetizing the inductor L_U is

$$T_7 = \sqrt{C_E L_U} = \frac{1}{\omega_7} = \frac{1}{\omega_6} \tag{21}$$

When i_{LU} reaches zero, the diodes of the snubber network turn off. The time necessary to feed back the stored energy is therefore

$$T_6 + T_7 = \left(\frac{\pi}{2}+1\right)\sqrt{C_E L_U} = \left(\frac{\pi}{2}+1\right) T_7 \tag{22}$$

Now the circuit is again in Mode 0!

III. Energy Recovery for the Turn-off Snubber

After turn off of the main switch S, the snubber capacitor C_E is charged to the output voltage U_{out}. At the begin of Mode 6 (or also Mode 5, but that is not important), the energy stored in C_E is

$$W_{CE} = \frac{C_E U_{out}^2}{2} \; . \tag{23}$$

Using a dissipative snubber this energy has to be dissipated in a resistor R_E. Then, with the switching frequency f, the loss would be

$$P_{RE} = \frac{C_E U_{out}^2}{2} f \; . \tag{24}$$

When the main switch S turns on again, the auxiliary switch S_U can be turned on as well (Mode 6). The capacitor C_E is discharged within a quarter of the period and the current reaches its maximum I_{LUmax} (Fig. 9). According Fig. 8, the circuit can be described by

$$L_U \frac{d i_{LU}}{d t} + \frac{1}{C_E}\int_0^t i_{LU}\, d t - U_{out} + V_D + R_{loss1}\, i_{LU} = 0 \, . \tag{25}$$

where V_D is the knee voltage of the diode D_U and R_{loss1} is the series equivalent resistance of the inductor L_U and of the capacitor C_E, resistances, the differential resistance of the diode D_U and the on-state resistance of the auxiliary switch S_U. Therefore, the current can be described by

$$i_{LU}(t) = \left(U_{out} - V_D\right)\cdot \alpha_1 \cdot \sin\omega_1 t \, . \tag{26}$$

where

$$\alpha_1 = 2\sqrt{\frac{C_E}{4L_U - R_{loss1}^2 C_E}}; \quad \omega_1 = \sqrt{\frac{1}{L_U C_E} - \frac{R_{loss1}^2}{4L_U^2}} \tag{27a, b}$$

The capacitor C_E is completely discharged, when the current reaches its maximum at T_x:

$$T_x = \frac{\pi}{2}\frac{1}{\omega_1} \tag{28}$$

The loss energy can be calculated by

$$W_{loss1} = \int_0^{T_x} R_{loss1}\, i_{LU}^2(t)\cdot d t \tag{29}$$

$$W_{loss1} = R_{loss1}\left(U_{out} - V_D\right)^2 \alpha_1^2 \, \frac{T_x}{2} \, . \tag{30}$$

Now, the diode D_E turns on (Mode 7) and the voltage across C_E is clamped. According Fig. 10, the circuit can be described by

$$L_U \frac{d i_{LU}}{d t} + 3V_D + R_{loss2}\, i_{LU} + U_{out} = 0 \; . \tag{31a}$$

with initial condition:

$$i_{LU}(0) = i_{LU}(T_x) = \left(U_{out} - V_D\right)\alpha_1 \, . \tag{31b}$$

where V_D is the knee voltage of the diodes D_E, D_U, and D_R, and R_{loss2} is the series equivalent resistance of the circuit consisting of the inductor L_U, the diodes D_E, D_U, and D_R and the main switch S.

Solving the differential equation leads to

$$i_{LU}(t) = -I_\infty + I_1 \exp\left(-\frac{t}{\tau}\right) \tag{32}$$

where

$$I_\infty = \frac{U_2 + 3V_D}{R_{loss2}}; \quad I_1 = i_{LU}(0) + I_\infty; \quad \tau = \frac{L_U}{R_{loss2}} \tag{33a, b, c}$$

The current decreases and reaches zero after T_y:

$$T_y = \tau \; \ln\left(\frac{I_1}{I_\infty}\right). \tag{34}$$

Now, the diodes turn off and the recuperation ends. The loss energy during Mode 7 can be calculated by

$$W_{loss2} = \int_0^{T_y} R_{loss2}\, i_{LU}^2(t)\cdot d t \tag{35}$$

$$W_{loss2} = R_{loss2}\left[I_\infty^2 \cdot T_y + 2I_\infty I_1\, \beta\, \tau + I_1^2\, \beta\, \frac{\tau}{2}\right] \tag{36}$$

where

$$\beta = \frac{U_{out} + 3V_D}{R_{loss2} i_{LU}(0) + U_2 + 3V_D} - 1 = -\frac{i_{LU}(0)}{I_1} \tag{37}$$

Therefore, the losses of the recuperation network are

[Downloaded from www.aece.ro on Thursday, July 03, 2025 at 19:04:12 (UTC) by 172.69.214.181. Redistribution subject to AECE license or copyright.]

$$P_{loss,rek} = f(W_{loss1} + W_{loss2}). \tag{38}$$

The recovered power which can be fed back P_{back} is

$$P_{back} = f\left[\frac{C_E U_{out}^2}{2} - (W_{loss1} + W_{loss2})\right]. \tag{39}$$

This calculation is comprehensive. To get a rough overview we can make some approximations.

IV. Approximate Estimation of the Fed Back Energy

For approximating the energy which is fed back, we use the idealized curves according (14), (18), (20), and (21) and we calculate the losses at the parasitic resistors. The knee voltage of the diodes shall be neglected, because it is small compared to the output voltage. With (14), and (18), for the loss energy during Mode 6 one can write

$$W_{loss1} = \int_0^{T_6} R_{loss1}\left[U_{out}\omega_6 C_E \sin(\omega_6 t)\right]^2 dt . \tag{40}$$

One gets

$$W_{loss1} = \frac{\pi}{4} U_{out}^2 \ R_{loss1}\sqrt{\frac{C_E}{L_U}}\ C_E . \tag{41}$$

During Mode 7, with (20) and (22), one can write for the loss energy

$$W_{loss2} = \int_0^{T_7} R_{loss2}\frac{U_{out}^2}{L_U^2}(T_7 - t)^2\ dt . \tag{42}$$

$$W_{loss2} = \frac{1}{3} U_{out}^2 \ R_{loss2}\sqrt{\frac{C_E}{L_U}}\ C_E . \tag{43}$$

The losses of the recuperation network can be approximated by:

$$P_{loss} = f\cdot U_{out}^2\sqrt{\frac{C_E}{L_U}}\ C_E\left(\frac{\pi}{4}R_{loss1} + \frac{1}{3}R_{loss2}\right) . \tag{44}$$

Considering the same equivalent loss resistance for both modes, the recovered power P_{back} can be expressed as:

$$P_{back} = f\cdot\frac{C_E U_{out}^2}{2}\left(1 - 2.23 R_{loss}\sqrt{\frac{C_E}{L_U}}\right). \tag{45}$$

With the image impedance of the resonant circuit

$$Z_U = \sqrt{\frac{L_U}{C_E}} \tag{46}$$

we can write now:

$$P_{back} = f\cdot\frac{C_E U_{out}^2}{2}\left(1 - 2.23\frac{R_{loss}}{Z_U}\right). \tag{47}$$

The image impedance of the resonant circuit Z_U is large compared to R_{loss}, therefore a large amount of the stored energy of the snubber capacitor can be fed into the output of the converter.

V. Optimized Control of the Recuperation

A little bit more efficient way to control the recuperation network is to turn off the auxiliary switch S_U at the moment when the voltage across the capacitor C_E has such a value, that the capacitor will be completely discharged when the current i_{LU} reaches zero and the diodes turn off.

When the auxiliary switch is turned off after T_z, then, according to (14) and (15), the current in L_U and the voltage across C_E are, respectively:

$$i_{LU}(T_z) = U_{out}\omega_6 C_E \sin\omega_6 T_z \tag{48}$$

$$u_{CE}(T_z) = U_{out}\cos\omega_6 T_z . \tag{49}$$

If the auxiliary switch is turned off after

$$T_z = \frac{\pi}{3}\sqrt{C_E L_U} = \frac{\pi}{3}T_7 , \tag{50}$$

the mode that follows is described by KVL according to:

$$L_U\frac{di_{LU}}{dt} + U_{out} + \frac{1}{C_E}\int_0^t i_{LU}dt = u_{CE}(T_z) \tag{51}$$

with initial conditions:

$$i_{LU}(T_z) = i_{LU}\left(\frac{\pi}{3}T_7\right) = \frac{\sqrt{3}}{2}U_{out}\ \omega_6 C_E \tag{52}$$

$$u_{CE}(T_z) = u_{CE}\left(\frac{\pi}{3}T_7\right) = \frac{1}{2}U_{out} . \tag{53}$$

Solving the differential equation leads to:

$$i_{LU}(t) = u_a\sqrt{\frac{C_E}{L_U}}(\sin\omega_6 t) + i_{LU}(T_z)(\cos\omega_6 t) \tag{54}$$

$$u_{CE}(t) = +u_{CE}(T_z) - u_a\ (1-\cos\omega_6 t) - i_{LU}(T_z)\sqrt{\frac{L_U}{C_E}}(\sin\omega_6 t) \tag{55}$$

with

$$u_a = u_{CE}(T_z) - U_{out} . \tag{56}$$

The voltage across C_E and the current through the inductor L_U are zero after

$$T_z = \frac{\pi}{3}\sqrt{C_E L_U} = \frac{\pi}{3}T_7 . \tag{57}$$

Due to the fact that the current is smaller, the losses are a little bit smaller too. The auxiliary switch has to be turned off when the voltage across the snubber capacitor is half of the output voltage. This can be detected by a comparator. It makes especially sense when the capacitor is not over-charged. To avoid ringing when a turn-on inductor L_E is used, a switch in series to L_E can be included leading to modifications shown also in [15]. This reduces ringing during turn-off and enables an optimal feed-back of the energy, when the snubber capacitor is overcharged. This will be shown in a future paper.

VI. Influence of the Parasitic Capacitor of the Active Switch

In previous chapters, we studied only the main effect and used only the parameters L_E, D_E, and C_E of the network. When the voltage across the switch reaches the output voltage U_{out}, the free-wheeling diode D turns on. Considering the circuit consisting of the parasitic capacitance of the active switch C_S, the snubber capacitor C_E, and the snubber inductor L_E we get for the current i_{LE}, the current in the main diode D, and the voltage across the switch

$$i_{LE}(t) = I\cdot\cos\sqrt{\frac{1}{(C_E + C_S)L_E}}\cdot t \tag{58}$$

$$i_D(t) = I - i_{LE}(t) = I\cdot\left(1 - \cos\sqrt{\frac{1}{(C_E + C_S)L_E}}\cdot t\right) \tag{59}$$

[Downloaded from www.aece.ro on Thursday, July 03, 2025 at 19:04:12 (UTC) by 172.69.214.181. Redistribution subject to AECE license or copyright.]

$$u_S(t) = I\sqrt{\frac{L_E}{C_E + C_S}} \cdot \sin\sqrt{\frac{1}{(C_E + C_S)L_E}} \cdot t + U_2 \ . \tag{60}$$

The overshot is reduced to

$$\Delta u_S = I\sqrt{\frac{L_E}{C_E + C_S}} \ . \tag{61}$$

The snubber diode D_E turns off and there is now a ringing between L_E and C_S with the frequency

$$f_R = \frac{1}{2\pi} \cdot \sqrt{\frac{1}{C_S L_E}} \tag{62}$$

and with the reduced amplitude Δu_S.

One can see, that the inductor L_E should be dimensioned as small as possible when the presented low-loss snubber concept is used.

VII. Design Equations

A. *Dimensioning of the basic boost converter*

The boost converter shall transform a 50 V input voltage into an output voltage of 150 V. The rated power is 500 W. The output ripple shall be about 3%. The mean value of the input current is therefore 10 A (omitting the losses). The current ripple is chosen to 5 A. The inductor can be determined by the basic equation of the inductor with the input voltage U_{in}, the on-time of the active switch d_cT (with d_c as the duty cycle and T as the switching period), and the current ripple ΔI

$$L = \frac{U_{in} \cdot d_c T}{\Delta I} = \frac{U_1 \cdot d_c}{\Delta I \cdot f} \tag{63}$$

To get an approximate value for the output capacitor C we use the fact that during the on-time of the active switch the load has to be supplied by the capacitor. Therefore, the voltage across it decreases by ΔU_C. We get

$$C = \frac{I_{Load} \cdot d_c T}{\Delta U_C} = \frac{I_{Load} \cdot d_c}{\Delta U_C \cdot f} \tag{64}$$

This equation is derived for an ideal capacitor. In real cases, there is always a series resistor, which causes an additional voltage drop. So the value must be always chosen higher. With a chosen switching frequency of f = 50 kHz and an average output current of I_{Load} = 3,3 A one gets L = 130 µH, and C = 33 µF.

B. *Dimensioning of the snubber network*

To reduce the losses during turn-on an inductor L_E is connected in series with the active switch S. This defines the rise of current through the switch (and also the velocity of the current reduction in the diode D and therefore defines the reverse recovery peak). For a chosen value of the current rise $(di/dt)_{chosen}$ we get

$$L_E = \frac{U_2}{(di/dt)_{chosen}} \tag{65}$$

With $(di/dt)_{chosen}$ = 100 A/µs and an output voltage of 150 V, one gets L_E = 1,5 µH.

The snubber capacitor C_E has to limit the overvoltage during turn off caused by the inductor L_E (and to limit the rise of the voltage across the switch). The energy stored into L_E at the moment before turning off when the instantaneous current is I can be expressed as:

$$W_{LE} = \frac{L_E \cdot I^2}{2} \tag{66}$$

This energy has to be charged into the capacitor C_E when the voltage across it reaches U_2 and the free-wheeling diode turns on (not considering the possible current path over L_U). Due to the delayed commutation into the free-wheeling diode further energy is transferred into the snubber capacitor C_E. With a chosen value of the overvoltage $(\Delta U)_{chosen}$ one gets:

$$C_E = \frac{I^2}{(\Delta U)^2_{chosen}} L_E \ . \tag{67}$$

With I = 12 A and $(\Delta U)_{chosen}$ = 50 V, we obtained C_E = 81 nF.

With (22) it results

$$L_U = (T_6 + T_7)^2 \frac{4}{(2+\pi)^2 C_E} \tag{68}$$

So (T_6+T_7) must be smaller than the on-time of the active switch to ensure that the energy is completely fed back

$$(T_1 + T_2) < T_{on} = d_c T \tag{69}$$

For the simulation, we used L_U = 300 µH.

VIII. Results

A simulation was performed by LT-Spice and a small converter was bread-boarded. The results show a good conformity with the theory. Fig. 11 shows the control signal of the main switch, the control signal of the auxiliary switch, the voltage across the snubber capacitor C_E, and the current through the inductor L_U.

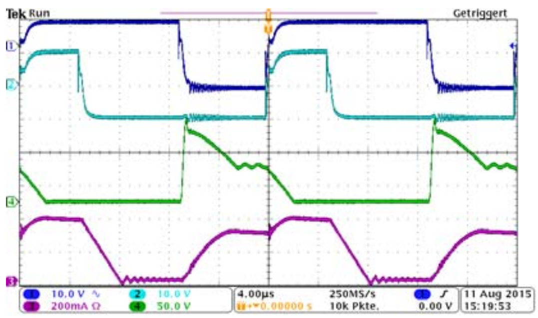

Figure 11. Control signal of the main switch, control signal of the auxiliary switch, voltage across snubber capacitor C_E, and current through the inductor L_U (top to down).

In Fig. 12, the control signals and the current through the main inductor, and the input current of the converter are shown.

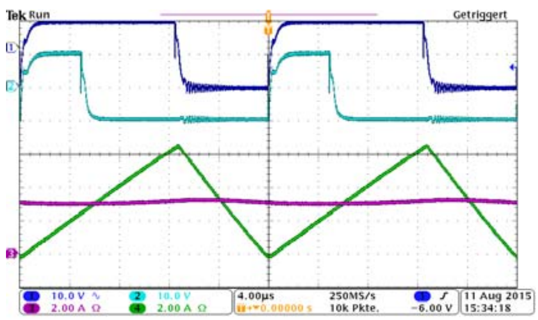

Figure 12. Control signal of the main switch, control signal of the auxiliary switch, current through the main inductor L, and input current (top to down).

[Downloaded from www.aece.ro on Thursday, July 03, 2025 at 19:04:12 (UTC) by 172.69.214.181. Redistribution subject to AECE license or copyright.]

The input current is nearly constant due to a capacitor between the input connectors.

IX. Conclusion

A boost converter with zero voltage turn-off and zero-current turn-on of the main switch was presented. With the help of a resonant circuit, two diodes and an auxiliary switch the energy stored in the snubber capacity is transferred to the output. To avoid ringing when a turn-on inductor L_E is used, a switch in series to L_E can be included leading to modifications. This reduces ringing during turn-off and enables an optimal feed-back of the energy, when the snubber capacitor is overcharged. The proposed circuit improves the efficiency if a snubber is necessary, e.g. because of EMC problems, and then it has a better efficiency compared to a converter with RCD snubber. The converter is useful for solar application, battery chargers and so on.

References

[1] Ned Mohan, Tore M. Undeland, William P. Robbins: "Power Electronics, Converters, Applications and Design," pp. 52-74, 3nd ed. New York: W. P. John Wiley & Sons, 2003.

[2] Yuriy Rozanov, Sergey Ryvkin, Evgeny Chaplygin, Pavel Voronin, "Power Electronics Basics," CRC Press, 2016.

[3] Kwang-Hwa Liu, Fred C. Lee, "Resonant switches - A unified approach to improve performance of switching converters," Proc. IEEE Int. Telecom. Energy Conf. INTELEC, pp. 344-351, 1984. doi:10.1109/INTELEC.1984. 4794149.

[4] Kwang-Hwa Liu, Ramesh Oruganti, Fred C. Lee, "Quasi-resonant converters - Topologies and Characteristics," IEEE Trans. on Power Electronics, Vol. PE-2, Issue. 1, pp. 62-71, 1987. doi:10.1109/TPEL.1987.4766333.

[5] Guichao Hua, Eric X. Yang, Yimin Jiang, Fred C. Lee, "Novel Zero-Current-Transition PWM Converters," IEEE Trans. on Power Electronics, Vol. 9, Issue 6, pp. 601-606, 1994. doi:10.1109/63.334775.

[6] Ching-Jung Tseng, Chern-Lin Chen, "Novel ZVT-PWM Converters with Active Snubbers," IEEE Trans. on Power Electronics, Vol. 13, Issue 5, pp. 861-869, 1998. doi:10.1109/63.712292.

[7] Carlos Marcelo de Oliveira Stein, H.L. Hey, "A True ZCZVT Commutation Cell for PWM Converters," IEEE Trans. on Power Electronics, Vol. 15, Issue 1, pp. 185-193, 2000. doi:10.1109/63.817376.

[8] Dong-Yun Lee, Min-Kwang Lee, Dong-Seok Hyun, Ick Choy, "New Zero-Current-Transition PWM DC/DC Converters Without Current Stress," IEEE Trans. on Power Electronics, Vol. 18, Issue 1, pp. 95-104, 2002. doi:10.1109/TPEL. 2002.807206.

[9] Chien-Ming Wang, "Novel Zero-Voltage-Transition PWM DC-DC Converters," IEEE Trans. on Industrial Electronics, Vol. 53, Issue 1, pp. 254-262, 2005. doi:10.1109/TIE.2005.862253.

[10] Pritam Das, Gerry Moschopoulos, "A Comparative Study of Zero-Current-Transition PWM Converters," IEEE Trans. on Industrial Electronics, Vol. 54, Issue 3, pp. 1319-1328, 2007. doi:10.1109/TIE.2007.891663.

[11] Sang-Hoon Park, So-Ri Park, Jae-Sung Yu, Yong-Chae Jung, Chung-Yuen Won, "Analysis and Design of a Soft-Switching Boost Converter With an HI-Bridge Auxiliary Resonant Circuit," IEEE Trans. on Power Electronics, vol. 25, Issue 8, pp. 2142-2149, 2010. doi:10.1109/TPEL.2010.2046425.

[12] Doo-Yong Jung, Young-Hyok Ji, Sang-Hoon Park, Yong-Chae Jung, Chung-Yuen Won, "Interleaved Soft-Switching Boost Converter for Photovoltaic Power-Generation System," IEEE Trans. on Power Electronics, Vol. 26, Issue 4, pp. 1137-1145, 2011. doi:10.1109/TPEL.2010.2090948.

[13] Nikhil Jain, Praveen K. Jain, Geza Joos, "A Zero Voltage Transition Boost Converter Employing a Soft-Switching Auxiliary Circuit With Reduced Conduction Losses," IEEE Trans. on Power Electronics, Vol. 19, Issue 1, pp. 130-139, 2004. doi:10.1109/TPEL.2003.820549.

[14] Nihal Altintaş, A. Faruk Bakan, Ismail Aksoy, "A Novel ZVT-ZCT-PWM Boost Converter," IEEE Trans. on Power Electronics, Vol. 29, Issue 1, pp. 256-265, 2014. doi: 10.1109/TPEL.2013.2252197.

[15] Wannian Huang, Xing Gao, Sondeep Bassan, Gerry Moschopoulos, "Novel dual auxiliary circuits for ZVT-PWM converters," Can. Journal of Elec. Comp. Eng., vol. 33, pp. 153-160, 2008. doi:10.1109/TPEL.2010.2046425.

[16] Mihai Lucanu, Ovidiu Ursaru, Cristian Aghion, Nicolae Lucanu, "Single-Phase Direct AC-AC Boost Converter," Advances in Electrical and Computer Engineering, vol. 14, Nr. 3, pp. 107-112, 2014. doi:10.4316/AECE.2014.03014.

[17] Srdjan Srdic, Zeljho Despotovic, "A Buck-Boost Converter Modified to Utilize 600V GaN Power Devices in a PV Application Requiring 1200V Devices," Advances in Electrical and Computer Engineering, vol. 15, nr. 3, pp. 59-64, 2015. doi: 10.4316/AECE.2015.03008.

[18] Daniel Draghici, Dan Lascu, "Predictive Trailing-Edge Modulation Average Current Control in DC-DC Converters," Advances in Electrical and Computer Engineering, vol. 13, Nr. 4, pp. 111-116, 2013. doi: 10.4316/AECE.2013.04019.

[19] Zhe Zhang, M.A.E. Andersen, "Interleaved boost-half-bridge dual-input DC-DC converter with a PWM plus phase-shift control for fuel cell applications," Proc. 39th Annual Conference of the IEEE Industrial Electronics Society, IECON 2013, pp. 1679 – 1684, 2013. doi:10.1109/IECON.2013.6699385.

[20] Z. Salam, S.M. Ayob, M.Z. Ramli, N.A. Azli, "An Improved DC-DC Type High Frequency Transformer-Link Inverter by Employing Regenerative Snubber Circuit," Proc. 7th International Conference on Power Electronics and Drive Systems PEDS '07, pp. 1081 - 1084, 2007. doi:10.1109/PEDS.2007. 4487838.

[21] Felix A. Himmelstoss: Combined Low-Loss Switching Relieve (Kombinierte verlustarme Ein-Ausschaltentlastung), Austrian patent AT 505802 B1, 15.2.2010.

[22] Douglas G. Fent, "An Automatic Universal Boost Charging Algorithm for Lead Acid Batteries," Proc. of the first Int. Telecom. Energy Special Conference, TELESCON '94, pp. 453-456, 1994. doi:10.1109/TELESC.1994.4794375.

[23] Dorin Petreus, Daniel Moga, Adina Rusu, Toma Patarau, Mihai Munteanu, "Photovoltaic System with Smart Tracking of the Optimal Working Point," Advances in Electrical and Computer Engineering, vol. 10, Nr. 3, pp. 40-47, 2010. doi: 10.4316/AECE.2010.03007.

[24] Jan Vittek & Stephen J. Dodds, "Forced Dynamics Control of Electric Drives," EDIS-Zilina University publisher, ISBN 80-8070-087-7, 2003.